Electrophysiological and molecular characterization of the inward rectifier in juxtaglomerular cells from rat kidney

Anke Leichtle[1], Ulrich Rauch[1], Margitta Albinus[1], Peter Benöhr[1], Hubert Kalbacher[2], Andreas F. Mack[3], Rüdiger W. Veh[4], Ulrich Quast[1] and Ulrich Russ[1]

[1] *Department of Pharmacology and Toxicology, Medical Faculty, University of Tübingen, Wilhelmstrasse 56, D-72074 Tübingen, Germany*
[2] *Department of Physiological Chemistry, Hoppe-Seyler-Strasse 4, D-72076 Tübingen, Germany*
[3] *Department of Anatomy, Medical Faculty, University of Tübingen, Österbergstrasse 3, D-72074 Tübingen, Germany*
[4] *Department of Anatomy, Charité, Philippstrasse 12, D-10098 Berlin*

Renin, the key element of the renin–angiotensin–aldosterone system, is mainly produced by and stored in the juxtaglomerular cells in the kidney. These cells are situated in the media of the afferent arteriole close to the vessel pole and can transform into smooth muscle cells and vice versa. In this study, the electrophysiological properties and the molecular identity of the K^+ channels responsible for the resting membrane potential (~ -60 mV) of the juxtaglomerular cells were examined. In order to increase the number of juxtaglomerular cells, afferent arterioles from NaCl-depleted rats were used, and $>90\%$ of the afferent arterioles were renin positive at the distal end of the arteriole. Whole-cell and cell-attached single-channel patch-clamp experiments showed that juxtaglomerular cells are endowed with a strongly inwardly rectifying K^+ channel (Kir). The channel was highly sensitive to inhibition by Ba^{2+} (inhibition constant 37 μM at 0 mV), but relatively insensitive to Cs^+ and, with 142 mM K^+ in the pipette, had a single-channel conductance of 31.5 pS. Immunocytochemical studies showed the presence of Kir2.1 but no signal for Kir2.2 in the media of the afferent arteriole. In PCR analyses using isolated juxtaglomerular cells, the mRNA for Kir2.1 and Kir2.2 was detected. Collectively, the results show that Kir2.1 is the dominant component of the channel. The current carried by these channels plays a decisive role in setting the membrane potential of juxtaglomerular cells.

(Resubmitted 25 June 2004; accepted 28 July 2004; first published online 5 August 2004)
Corresponding author U. Russ: Department of Pharmacology and Toxicology, Medical Faculty, University of Tübingen, Wilhelmstrasse 56, D-72074 Tübingen, Germany. Email: ulrich.russ@uni-tuebingen.de

The renin–angiotensin–aldosterone system plays a dominant role in the control of blood pressure and electrolyte balance of the organism. The activity of this system is controlled by the aspartyl protease renin, which mostly stems from the juxtaglomerular myoepitheloid cells in the media of the afferent arteriole close to the entrance into the glomerulus (for review see Hackenthal *et al.* 1990). Smooth muscle cells and juxtaglomerular cells in the distal part of the afferent arteriole are linked by gap junctions (Taugner & Hackenthal, 1989) and show strong electrical coupling (Kurtz & Penner, 1989; Russ *et al.* 1999). Juxtaglomerular cells can transform into vascular smooth muscle cells and vice versa (Cantin *et al.* 1977; Sequeira Lopez *et al.* 2001) and the two cell types share many electrophysiological properties (Taugner & Hackenthal, 1989). The number of renin-positive arterioles and the number of juxtaglomerular cells within one arteriole are increased when high activity of the renin–angiotensin–aldosterone system is required, e.g. in case of a NaCl depletion (Taugner & Hackenthal, 1989).

Control of renin secretion from juxtaglomerular cells is complex, involving intrarenal mechanisms (e.g. the macula densa and the baroreceptor mechanisms) and extrarenal signals (e.g. from sympathetic nerves and circulating hormones; for review see Kurtz, 1989; Hackenthal *et al.* 1990; Osswald & Quast, 1995). An intriguing feature of the control of renin secretion is the 'Ca^{2+} paradox', i.e. the observation that manoeuvres that decrease the cytoplasmic Ca^{2+} concentration ($[Ca^{2+}]_i$) increase the rate of renin secretion from juxtaglomerular cells and vice versa (Kurtz, 1989; Hackenthal *et al.* 1990). Depolarization of juxtaglomerular cells leads to an increase of the cytoplasmic free calcium concentration (Russ *et al.* 1999) and to a decrease of the renin secretion (review in Kurtz, 1989). In non-pressurized afferent arterioles, the resting membrane potential of juxtaglomerular cells is

 DOI: 10.1113/jphysiol.2004.070359

~ -60 mV (Fishman, 1976 (two populations with -70 and -35 mV); Bührle *et al.* 1985; Russ *et al.* 1999; review in Kurtz, 1989); isolated juxtaglomerular cells from rat kidney are more depolarized (resting membrane potential -32 mV, Friis *et al.* 2003). In a pioneering study, Kurtz & Penner (1989), using mouse glomeruli with the distal part of the afferent arteriole attached, demonstrated a strongly inwardly rectifying K^+ conductance in juxtaglomerular cells, the activity of which determined the resting membrane potential. However, a more detailed electrophysiological characterization of this channel and of its molecular composition has not yet been undertaken.

In this study we have addressed these questions. In order to increase the number of renin-positive cells, intact afferent arterioles from NaCl-depleted rats were used. In particular the sensitivity of the Kir channel in juxtaglomerular cells to Ba^{2+} and Cs^+ and the single-channel conductance were determined; in addition, immunocytochemical and PCR experiments were performed to elucidate the molecular composition of the channel. We show that, also in rat juxtaglomerular cells, the activity of this channel determines membrane potential. The membrane potential of juxtaglomerular cells is directly or indirectly (i.e. via the cytoplasmic Ca^{2+} concentration) involved in the regulation of renin secretion (Kurtz, 1989; Persson, 2003) which, in turn, determines the activity of the renin–angiotensin system and thereby regulates blood pressure and electrolyte homeostasis.

Methods

Animals

Animal experimentation was conducted in accordance with the NIH Guide for the Care and Use of Laboratory Animals and German Law on the Protection of Animals. Sprague-Dawley rats (250–500 g) were used. To induce NaCl-depletion, animals were treated once with furosemide (10 mg kg^{-1}, I.P.) and kept on a NaCl-depleted diet (C1036, Altromin, Lage, Germany) for at least 2 weeks after furosemide application. Control animals were not treated with furosemide and were kept on a standard diet (C1324, Altromin).

Immunocytochemistry

The anti-renin antibody was produced by immunization of rabbits with a polypeptide comprising the amino acids 303–319 from rat renin conjugated to KLH-protein and the purified serum was used. Polyclonal antibodies against the less conserved C-terminus of the Kir2.1, Kir2.2 and Kir6.1 protein were raised in rabbits, and purified serum (Kir2.1) or affinity-purified antibodies (Kir2.2, Kir6.1) were used (Prüss *et al.* 2003; Thomzig *et al.* 2001, 2003). Tissue preparation for immunocytochemistry was done according to Pfaff *et al.* (1999). The animals were anaesthetized by intraperitoneal injection of thiopental sodium (Byk Gulden, Konstanz, Germany; 60 mg kg^{-1}) on the day of the experiment. After anaesthesia, the left cardiac ventricle was exposed through subcostal incision of the abdominal cavity and subsequent opening of the pericardium. The tip of a perfusion system was placed into the left ventricle, and the arterial system was perfused for 1 min with phosphate-buffered saline (PBS; 120 mM NaCl, 16 mM Na_2HPO_4, 2.9 mM KH_2PO_4) to clear the kidneys of blood and subsequently for 10 min with 150 ml of a fixation solution (4% paraformaldehyde and 3% sucrose in PBS). Both solutions were at room temperature. Kidneys were removed, cut into slices (3 mm in thickness) displaying cortex and outer and inner medulla, and incubated for 1 h in the fixation solution at 4°C. After rinsing 4 times in PBS for 15 min, kidney slices were cryoprotected by 30% sucrose in PBS for 12 h at 4°C, frozen in isopentane precooled by liquid nitrogen, and stored at -80°C until further use. Cryosections of approximately 16 μm were made at -20°C and transferred onto gelatin-coated glass slides. The following steps were performed at room temperature. After preincubation for 45 min in PBS containing 4% normal goat serum, 1% bovine serum albumin, and 0.25% Triton X-100 in PBS, sections were incubated for 4 h with the respective antibody (anti-Kir2.1 was diluted 1 : 50; anti-Kir2.2, 1 : 25; anti-Kir6.1, 1 : 50; anti-renin 1 : 100). After washing the sections three times for 5 min with PBS, they were incubated for 1.5 h with Alexa 488 goat anti-rabbit IgG (Molecular Probes, Eugene, OR, USA; final concentration, 13 μg ml^{-1}). Sections were then washed twice for 10 min in PBS and mounted in FluorSave (Calbiochem, San Diego, CA, USA) as a fading retardant. For immunocytochemical reference, cryosections of rat brain were prepared and stained with all Kir antibodies. Cryosections were analysed on a confocal microscope (LSM 410, Carl Zeiss, Oberkochen, Germany), using an Argon laser for excitation at a wavelength of 488 nm and appropriate filter sets. Optical section thickness for confocal fluorescence detection was set at approximately 0.8 μm, and non-confocal transmitted images were captured simultaneously in a separate detector. Five rats were used for tissue preparation and 38 (Kir2.1), 16 (Kir2.2) and 36 (Kir6.1) slices were evaluated.

Electrophysiology

Animals were killed by cervical dislocation, exsanguinated and the kidneys removed. A freshly isolated kidney was transferred in a Hepes-buffered physiological salt solution (PSS) containing (mM): NaCl 142, KCl 2.8, $MgCl_2$ 1, $CaCl_2$ 1, D(+)-glucose 11, buffered with Hepes (10 mM)

and titrated to pH 7.4 with NaOH at 37°C. The kidney was decapsulated, cut longitudinally into two halves and the isolated cortex was minced with a razor blade. Glomeruli were prepared by modifications of published methods (Kurtz & Penner, 1989; Metzger & Quast, 1996; Russ *et al.* 1999). The minced tissue was incubated for 50 min in 20 ml PSS with 20 mg collagenase A (Roche Diagnostics, Mannheim, Germany) at 37°C under gentle shaking. The suspension was then passed through stainless steel sieves of mesh 200 and 125 μm and the final material collected on a 63 μm sieve. Microscopic inspection showed that the preparations consisted mainly of glomeruli and some contamination with tubular fragments; about 10% of the glomeruli contained a remnant of the afferent arteriole up to 100 μm in length.

Glomeruli were transferred to the recording chamber equipped with a poly-L-lysin-coated cover slide. Electrophysiological recordings were taken from cells in the distal afferent arteriole close to the entrance into the glomerulus (Russ *et al.* 1999). The patch-clamp technique was used in the whole-cell (at 37°C) and cell-attached (at room temperature) configurations as described by Hamill *et al.* (1981). Bath solution was PSS in the whole-cell current-clamp and most cell-attached experiments or a high-K^+ solution (mM: KCl 142, NaCl 2.8, $MgCl_2$ 1, $CaCl_2$ 1, D(+)-glucose 11, Hepes 10, titrated to pH 7.4 with NaOH) in the whole-cell voltage-clamp and some cell-attached experiments. Patch pipettes were drawn from borosilicate glass capillaries (GC 150, Harvard Apparatus Ltd, Edenbridge, UK) and heat polished using a horizontal microelectrode puller (Zeitz, Augsburg, Germany). For whole-cell current-clamp experiments pipettes were filled with (mM) potassium glutamate 132, NaCl 10, $MgCl_2$ 2, Hepes 10, EGTA 1, Na_2ATP 1, titrated to pH 7.2 with NaOH. For whole-cell voltage-clamp experiments the pipette solution was slightly changed (mM: potassium glutamate 126, NaCl 10, $MgCl_2$ 4, Hepes 10, EGTA 1, Na_2ATP 3, titrated to pH 7.2 with NaOH). Potentials given in these experiments were corrected for a liquid junction potential of 10 mV (Neher, 1992). Single-channel activity was recorded using the cell-attached configuration with the high-K^+ solution in the pipette. Here, sampling frequency was 2000 Hz and the data were filtered with 1000 Hz. To compute the histograms showing the frequency distribution of the current amplitude, 10 s of the recording were analysed. A Gaussian function with two to four components was fitted to the data. For presentation of current traces, sample frequency was reduced to 200 Hz and filtered correspondingly.

Pipette resistance was always 3–5 MΩ. Data were recorded with an EPC 9 amplifier using Pulse software (HEKA, Lambrecht, Germany). Results are given as mean ± standard error of the mean.

PCR

RT-PCR was performed using RNA from isolated juxtaglomerular cells from rat kidney, prepared as described by Albinus *et al.* (1998), from rat kidneys and from brain. Total RNA was extracted using the peqGOLD RNAPure System (Peqlab, Erlangen, Germany) according to the manufacturer's protocol. The yield was determined spectrophotometrically at 260 nm and the integrity of the purified RNA was analysed by agarose gel electrophoresis. First strand cDNA was synthesized from 1 μg total RNA in a solution of 20 μl containing random primer (final concentration 10 mM; Promega, Mannheim, Germany), 1 mM dNTP, 250 ng oligo dT Primer (Promega), 5 mM $MgCl_2$, 20 units (U) RNAase inhibitor (Promega), 125 U AMV-reverse transcriptase (Peqlab) and 1 × PCR buffer (Pan Biotech, Aidenbach, Germany). The solution was incubated for 10 min at room temperature, then for 60 min at 42°C and finally for 3 min at 95°C. The PCR reaction mixture (50 μl) contained 15 μl of this cDNA solution, dNTP (0.2 mM), 2.5 U PAN^{TM}Script *Taq* polymerase (Pan Biotech), 1 × PCR buffer, and Kir2.x specific primers (50 nM). The primers were designed to amplify a 326 bp from the Kir2.1 and a 836 bp sequence from Kir2.2 channels, respectively (Kir2.1 sense nucleotides (nt) 864–883, and anti-sense, nt 1170–1189, gene accession no. GA L48490; Kir2.2 sense, nt 419–438, and anti-sense, nt 1235–1254, GA X78461; Bradley *et al.* 1999). PCR was performed for 2 min at 94°C, followed by 32 cycles of 1 min at 94°C, 30 s at 61°C and 1 min at 72°C, and finished with a final 10 min extension at 72°C. The reaction products were analysed by agarose gel electrophoresis and photographed. Cyclophillin (sense nt 159–178, anti-sense nt 397–415; GA M25637; 257 bp) was used as an internal control; for cyclophillin mRNA detection, 5 μl cDNA solution were used.

Results

Immunocytochemical localization of renin in slices from rat kidney

In a preliminary set of experiments we used neutral red to identify juxtaglomerular cells in afferent arterioles as described by Fishman (1976). However with this dye, which stains acidic cellular compartments, we found red vesicles in almost all cells of the afferent arteriole (see supplementary material available online only). More specifically the distribution of renin-secreting cells in rat kidney was characterized using a polyclonal antibody serum raised against rat renin. Figure 1*A* shows a typical section from a kidney slice prepared from a rat kept on a NaCl-depleted diet. The picture on the left shows the fluorescence signal from the renin antibody. In the overlay of the bright field pictures and the fluorescence image on the right one can see the glomerulus in the centre with the

afferent arteriole leading to the right. This overlay picture clearly identifies the terminal part of the afferent arteriole, i.e. the juxtaglomerular cells, as the major origin of the renin signal. Figure 1*B* illustrates the distribution of renin-positive vessel segments along afferent arterioles from NaCl-depleted and control rats. Close to the entrance of the afferent arteriole into the glomerulus, the probability of finding renin-positive cells was 93% for NaCl-depleted rats and 76% for control rats, respectively. With increasing distance from the glomerulus, there was a strong decrease in the number of renin-positive cells in both cases. NaCl depletion led to an increase in the number of renin-positive vessels and in the length of the renin-positive region ($P < 0.01$, Mann–Whitney rank sum test).

Electrophysiological experiments

For the experiments, bulgy roundish cells in the distal afferent arteriole were selected close to the entrance into the glomerulus, a region where in almost all vessels renin-secreting cells are located (see above; Fig. 1; Russ *et al.* 1999). These cells are clearly distinguished from smooth muscle cells which have a spindle-like appearance and a spiral arrangement around the vessel (Bührle *et al.* 1984; Hackenthal *et al.* 1990). First, the sensitivity of the membrane potential to Ba^{2+} was determined in whole-cell current-clamp experiments. Resting membrane potential was -63 ± 6 mV ($n = 6$). Addition of Ba^{2+} (100, 300 and 1000 μM) to the bath depolarized the cell by 6 ± 1, 10 ± 1 and 16 ± 1 mV, respectively (Fig. 2*A*; $n = 6$). Washout of Ba^{2+} restored the resting membrane potential.

Inhibition of whole-cell currents by Ba^{2+} was studied in voltage-clamp experiments with high-K^+ solution in the bath. Figure 2*B* shows that at very negative potentials, Ba^{2+} was a potent blocker of the inward currents and that the potency of block decreased at less negative potentials. The block was (essentially) reversible upon washout of Ba^{2+} ($n = 3$). For further evaluation of the voltage dependence of Ba^{2+} block, the currents during the last 20 ms of

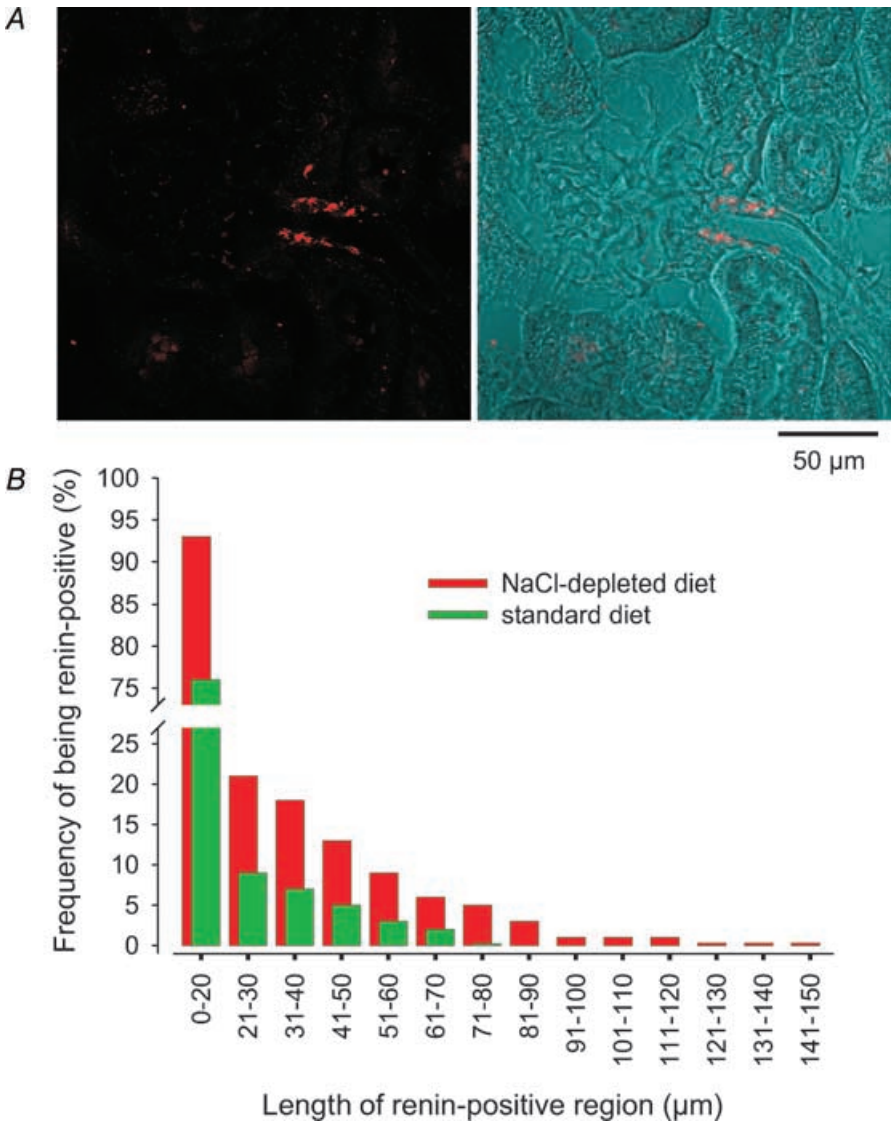

Figure 1. Immunocytochemical localization of renin in rat kidney slices
A, section from a kidney slice prepared from a NaCl-depleted rat. Left: fluorescence signal from renin antibody. Right: overlay of bright field and the fluorescence images. Visible is a glomerulus in the centre and the afferent arteriole at the right. The length of the renin-positive vessel segment was ~45 μm. *B*, probability of finding a renin-positive segment along the afferent arteriole from the vessel pole towards the proximal end for NaCl-depleted and control rats. 292/433 glomeruli were evaluated from 32/35 kidney slices from 4/4 animals (NaCl-depleted/control rats). Due to the two-dimensional nature of the pictures and the diameter of the vessel, the entrance of the afferent arteriole into the glomerulus cannot be precisely determined and the first segment of 20 μM was not subdivided further.

each pulse were averaged (Fig. 2*C*). From these data, concentration–inhibition curves were constructed at each voltage (not illustrated) and gave IC_{50} values of ~0.8, 1.4, 2.5, 5.0, 8.7 and 14.5 μM at −130, −110, −90, −70, −50 and −30 mV holding potential, respectively. Assuming a one-site model for Ba^{2+} block (Liu *et al.* 2001) and setting $IC_{50} = K_d$, a semilogarithmic plot of these data (Fig. 2*D*) gives a straight line and allows interpretation of the voltage dependence according to Woodhull (1973):

$$K_d = K_d(0) \exp(-\delta z F/RT)V$$

Here, $K_d(0)$ is the K_d value for Ba^{2+} at 0 mV; z, F, R and T have their conventional meaning and $V = E_{hold}$. δ denotes the fraction of the electric field sensed at the Ba^{2+} binding site. Linear regression of the data gave for $K_d(0)$ a value of 37 μM; from the slope, δ was calculated to 0.39. Positive to −10 mV a prominent current component was visible which was almost insensitive to 1 mM Ba^{2+} (Fig. 2*B* and *C*).

Membrane potential and whole-cell current were rather insensitive to Cs^+. In current-clamp experiments with PSS in the bath, Cs^+ (1 mM) showed no effect; at 5 mM, a small depolarization by ~2 mV was seen ($n = 3$; data not shown). In voltage-clamp experiments with high-K^+ bath solution, Cs^+ (50 μM) partially inhibited the current at −130 and −110 mV; at potentials positive to −90 mV, no inhibition was seen ($n = 4$; Fig. 3). Additionally, two other K^+ channel blockers, tedisamil and ciclazindol, were tested in whole-cell voltage-clamp experiments with high-K^+ solution in the bath (data not shown). In two

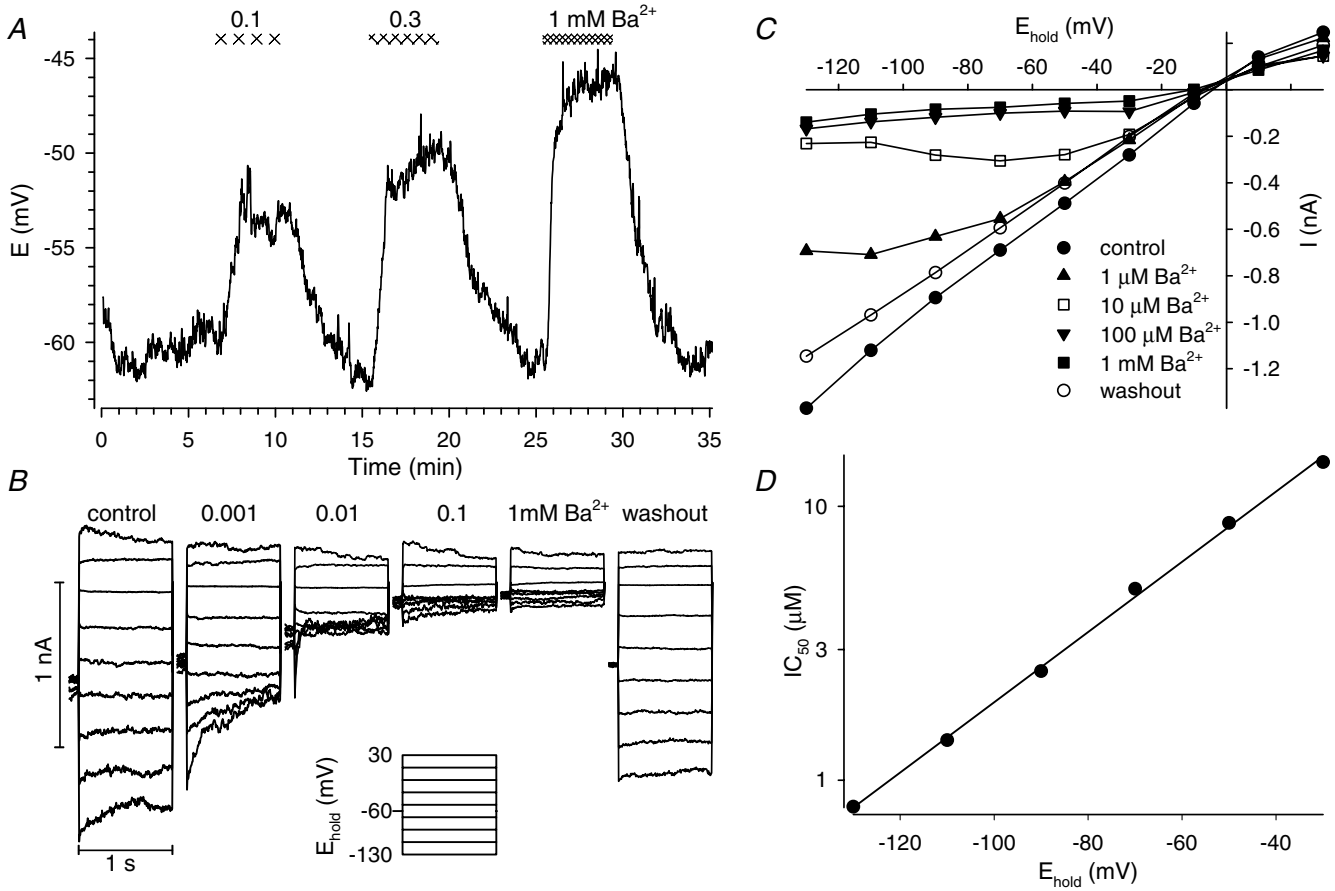

Figure 2. Sensitivity to Ba^{2+} of membrane potential and whole-cell current from juxtaglomerular cells
A, current-clamp experiment showing the depolarization of a juxtaglomerular cell induced by bath perfusion with Ba^{2+} (0.1, 0.3 and 1 mM). The effect of Ba^{2+} was rapidly reversed upon removal of the blocker from the bath. *B*, voltage-clamp experiment with high potassium solution in the bath illustrating the voltage-dependent inhibition of the whole-cell inward current by Ba^{2+}. The voltage jump protocol is shown in the inset. At −130 and −110 mV, Ba^{2+} (1 μM) essentially abolished the current; around physiological potentials (−50 to −30 mV), Ba^{2+} (0.1 and 1 mM) still induced inhibition. The Ba^{2+} block was (essentially) reversible upon washout. Note the disappearance of the small depolarization-induced (voltage-dependent) outward current at +30 mV with time. *C*, concentration dependence of the Ba^{2+}-induced current inhibition. The last 20 ms of the currents at each Ba^{2+} concentration are plotted against the clamp potential. The voltage dependence of the inhibition is most prominent at 1 and 10 μM Ba^{2+}. *D*, Woodhull analysis of the voltage dependence of Ba^{2+} block. Plotting the IC_{50} values on a logarithmic scale *versus* test potential gave a linear relationship (see text).

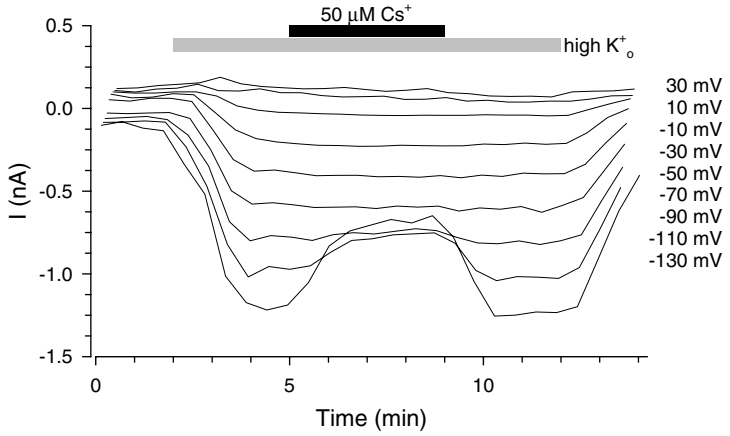

Figure 3. Sensitivity of whole-cell current from juxtaglomerular cells to Cs^+
Exchange of the standard Na^+-based bath solution (PSS) by a buffer with high K^+ induced strong inward currents. At −130 and −110 mV, these currents were inhibited by Cs^+ (50 μM); at clamp potentials positive to −90 mV, no inhibition was observed.

patches, 10 μM tedisamil showed no or a very small effect on the inwardly rectifying current; at 100 μM, a slow inhibition was seen which reached about 30% after 10 min ($n = 3$) and which was partially reversible. Ciclazindol was somewhat more potent; 10 and 100 μM reversibly inhibited about 10 and 50% of the current, respectively ($n = 3$). Inhibition by both drugs was restricted to inward currents (i.e. at negative potentials) and was independent of voltage within this range.

To gain further information on the channel underlying the observed current, single-channel recordings were made (Fig. 4). In the cell-attached configuration with high-K^+ solution in the pipette, but with standard Na^+-rich buffer in the bath, in 11 patches one dominating type of channel was detected. Channel activity was restricted to negative clamp potentials. To evaluate the single-channel conductance, all point histograms were generated and the distribution maxima were determined by fitting Gaussian-functions to the data. Figure 5*A* shows the histogram constructed from the recording at −90 mV shown in Fig. 4. The difference between the maxima of the histogram (at the respective test potential) was then plotted against the test potential (Fig. 5*B*) and linear regression analysis was performed, giving a single-channel conductance of $\gamma = 31.5 \pm 0.6$ pS ($n = 11$).

In another set of experiments we tested whether or not the expression of this inwardly rectifying 31.5 pS channel was modified by the Na^+-restricted diet of the animals. Therefore, afferent arterioles were prepared from rats on normal and NaCl-restricted diets, and single-channel experiments were performed as before. No difference between the two preparations was found (data not shown); however, in this set of experiments with both preparations strongly depolarized positive to +80 mV, a channel was sometimes seen with a single-channel conductance of ∼180 pS. Further experiments were

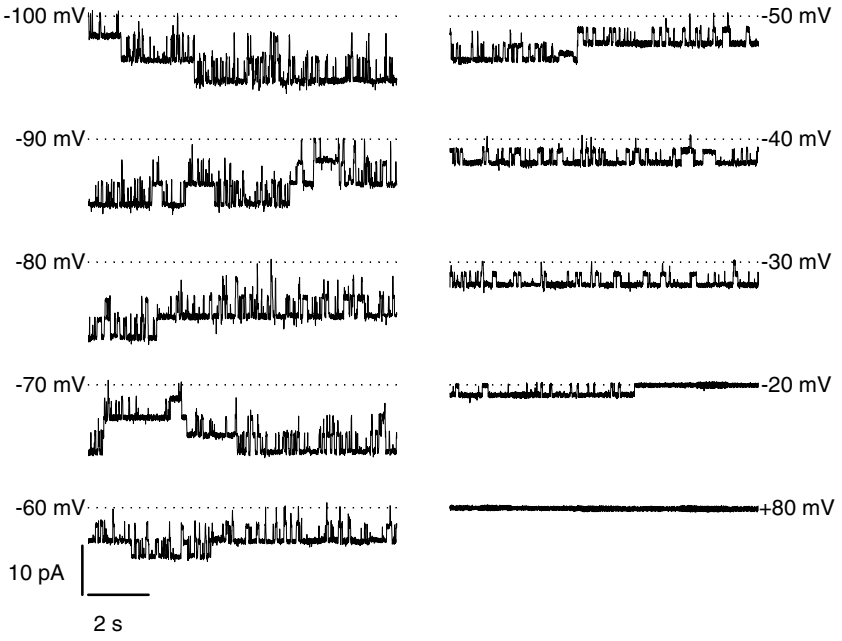

Figure 4. Single-channel recording in the cell-attached configuration
Consecutive recordings of 10 s each from the same patch at different test potentials are presented with high-K^+ solution in the pipette, but standard Na^+-rich bath solution; the dotted line indicates the closed level. At least 4 channels were present in the patch. No channel activity was seen at +80 mV. The apparent decrease in channel activity at lower voltages was observed only in this patch.

conducted in which the K^+-rich solution used for filling of the pipette was also present in the bath. Figure 6 shows recordings from juxtaglomerular cells from a rat fed on the standard diet. At negative clamp potentials, observations were very similar to those shown in Fig. 4; however, the reversal potential was shifted to ~ -15 mV (Fig. 6). At clamp potentials positive to +40 mV, the large-conductance channel was regularly seen and channel activity increased continuously with increasing depolarization up to +100 mV (higher potentials were not applied). At potentials positive to +80 mV, single-channel currents deviated from Ohmian behaviour (Fig. 6) and these values were not used for calculation of the single-channel conductance, which gave a value of 177 pS. The reversal potential of the channel, if calculated from the data up to +80 mV, was almost identical to that obtained for the 31.5 pS inwardly rectifying channel (Fig. 6). The differences between the reversal potentials in K^+-rich and Na^+-rich bath solution (Fig. 4) point to a depolarization of the cells by ~50 mV if the K^+-rich solution is applied. No obvious differences were observed in this series of experiments between control animals (15 patches from 4 rats) and rats fed on a Na^+-restricted diet (10 patches from 2 rats).

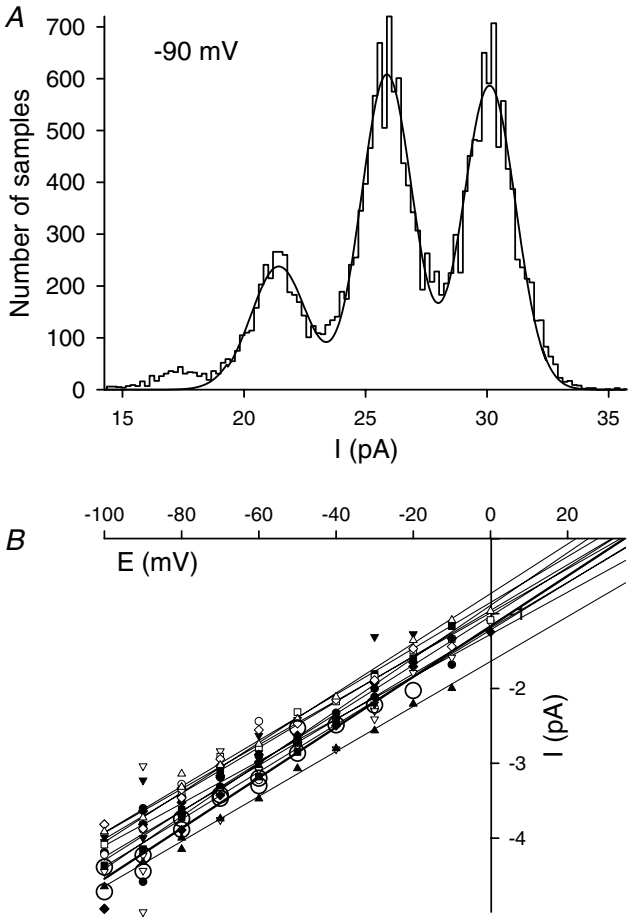

Figure 5. Single-channel current–voltage relationship
A, all-point histogram constructed from the recording at −90 mV shown in Fig. 4 (bin-width was 195 fA). The closed current level (at ~17.7 pA, no correction for current offset) and three open current levels are clearly visible. Three independent Gaussian-functions were fitted to the data (using 70 bins from 19.3 to 33.0 pA; continuous line), giving differences of 4.4 and 4.2 pA, respectively, between the maxima. *B*, current–voltage relationship. The differences in conduction levels constructed from 11 independent experiments are plotted against the test potential; the results from the experiment shown in Fig. 4 are represented by large open circles. Linear regression of the data is displayed by the straight lines with the bold line representing the linear regression of the data from Fig. 4. The offset of the current–voltage relationships (with a zero current potential of 34.8 ± 2.8 mV calculated from the 11 regression lines) is due to the membrane potential of the cell in the Na^+-rich bath solution.

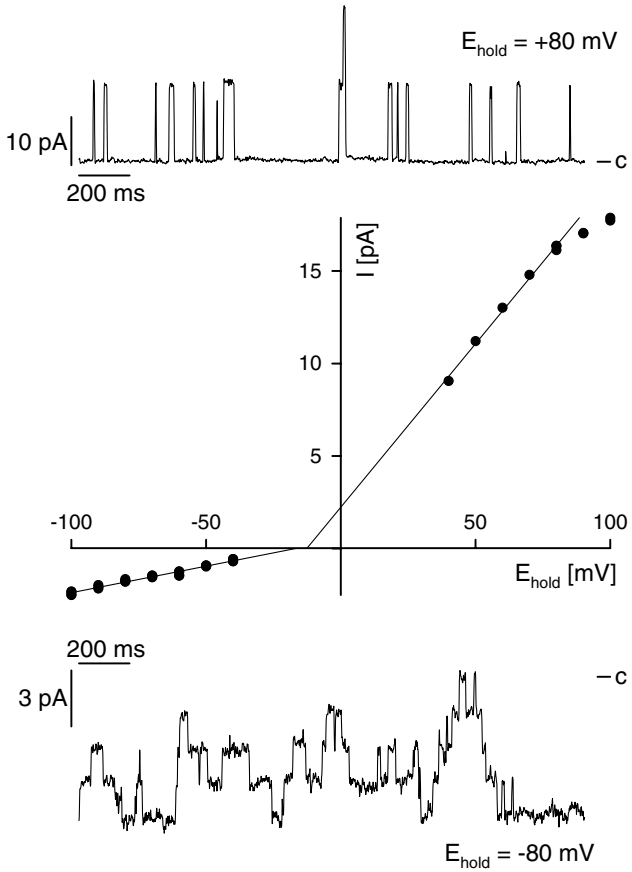

Figure 6. Single-channel recording in a K^+-rich bath solution
Recordings are from a single experiment using an afferent arteriole from a control rat on standard diet. In contrast to the data shown in Figs 4 and 5, the bath was also filled with the high-K^+ buffer used for filling the pipette. The upper trace shows a recording at +80 mV with at least 2 channels active in the patch. Linear regression of the single-channel currents from +40 to +80 mV gave a single-channel conductance of 177 pS and a reversal potential of −13 mV. The lower trace shows a recording at −80 mV with at least 4 active channels in the patch. Linear regression of the single-channel currents from −40 to −100 mV gave a single-channel conductance of 29 pS and a reversal potential of −17 mV. 'c' indicates the closed level.

Immunocytochemistry and PCR

Using polyclonal antibodies against Kir2.1 and 2.2, the localization of these channel proteins was analysed in slices from rat kidney; rat brain slices were stained as a control. Figure 7 shows that the Kir2.1 antibody gave a strong signal in the juxtaglomerular region of the afferent arteriole; furthermore, Kir2.1 was also found in the proximal part of the tubulus (data not shown). For Kir2.2, no signal was detected in the kidney. Using an antibody against Kir6.1, the pore-forming subunit of K_{ATP} channels in vascular smooth muscle cells, the juxtglomerular region of the afferent arteriole was strongly labelled, similar to the observations with the Kir2.1 antibody. All three antibodies gave clear and typical signal patterns in brain tissue slices (supplementary material which can be found online) similar to those obtained by other groups (Prüss *et al.* 2003).

RT-PCR was performed with mRNA extracted from isolated juxtaglomerular cells (Albinus *et al.* 1998), from whole kidney and, as a control, from whole rat brain. Using specific primers for Kir2.1 and Kir2.2 (see Methods, Bradley *et al.* 1999), mRNA of the expected size (326 bp for Kir2.1 and 836 bp for Kir2.2, respectively) was present in all samples tested (Fig. 8). Cyclophillin was used as house-keeping gene.

Discussion

In this study we have characterized the inwardly rectifying K^+ channel in rat juxtaglomerular cells using electrophysiological techniques and have attempted to determine the molecular identity by immunocytochemistry and PCR. The results of this study are in contrast to the recent report of Friis *et al.* (2003), who did not detect an inwardly rectifying K^+ current in isolated juxtaglomerular cells from rat kidney. The preparations used in the two studies are different (afferent arteriole mainly from rats on a NaCl-restricted diet *versus* isolated juxtaglomerular cells prepared from rats on a normal diet) and we will discuss first whether these methodological differences can explain the discrepancy.

Identity of cells selected for electrophysiological experiments and electrical coupling

The tunica media of the distal part of the afferent arteriole contains both smooth muscle and juxtaglomerular cells; hence, the first question arising is that of the identity of the cells examined. Juxtaglomerular cells can be metaplastically transformed to smooth muscle cells and vice versa (Cantin *et al.* 1977; Sequeira Lopez *et al.* 2001) and differences in the channel equipment of the two cell types may occur. As an example, vascular smooth muscle cells are endowed with voltage-dependent Ca^{2+} channels whereas juxtaglomerular cells are not (Kurtz *et al.* 1990; Scholz & Kurtz, 1995); however, evidence for the existence of such channels on rat isolated juxtaglomerular cells has recently been presented (e.g. Friis *et al.* 2003). In experiments using sharp microelectrodes, no differences in membrane potential between smooth muscle and granulated cells in the afferent arteriole were detected, nor were there different responses to several neurotransmitters and hormones between the cell types (Taugner & Hackenthal, 1989).

Unambiguous identification of a juxtaglomerular cell in electrophysiological experiments may be difficult; however, two points suggest that generally juxtaglomerular cells were selected. First, only roundish protruding cells were used for patch clamping, and these are more likely to be juxtaglomerular cells than the spindle-like smooth muscle cells. Second, afferent arterioles from salt-depleted rats were used; in this case, $> 90\%$ of the afferent arterioles were renin positive at the vessel pole (Fig. 1; see also Taugner & Hackenthal, 1989). The experiments identifying Kir (Figs 4 and 5) were performed using

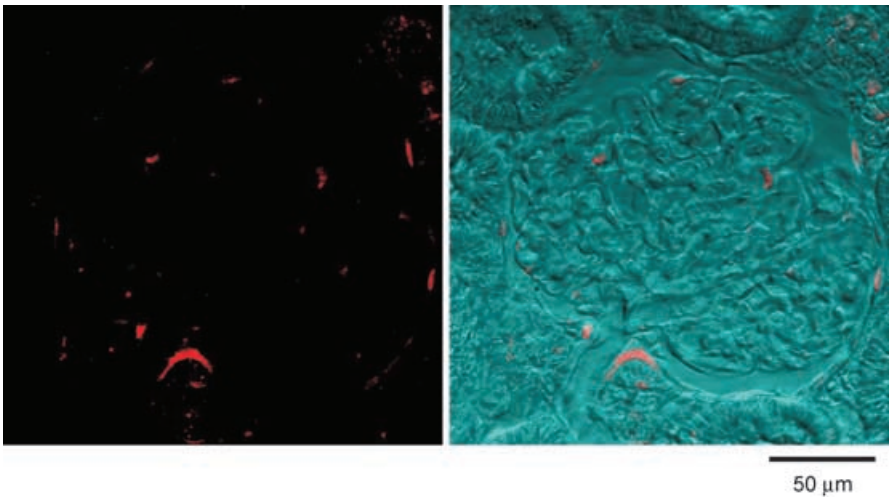

Figure 7. Immunocytochemical localization of Kir2.1
Section through the cortex of a rat kidney. Left: fluorescence image after immunostaining with a Kir2.1 antibody. Right: overlay of the fluorescence and the bright field images. The glomerulus with the afferent arteriole is clearly visible. The most prominent fluorescence signal originates from the vessel pole. In addition, there is some staining within the glomerulus and at the capsule wall (probably epithelial cells), and from the proximal vessel wall.

11 cells and gave reproducible results; it is therefore extremely unlikely that by chance in these 11 cases exclusively vascular smooth muscle cells were studied. This observation was confirmed by a second set of experiments with afferent arterioles from control rats (15 patches) and NaCl-depleted rats (10 patches).

A further complexity arises from the fact that cells in the distal part of the afferent arteriole are strongly electrically coupled (Kurtz & Penner, 1989; Russ *et al.* 1999), resulting in synchronized electrophysiological behaviour of the tissue. Hence, if a juxtaglomerular cell was selected, neighbouring smooth muscle cells may have contributed to the observed response. Whereas this may play a role for the results from experiments in the whole-cell mode (Figs 2 and 3, Ba^{2+} and Cs^{+} effects), it does not apply for the single-channel experiments performed in the cell-attached mode (Figs 4–6) and in which the current–voltage relationship and the single-channel conductance of Kir2 were determined (see below).

Juxtaglomerular cells from rats on NaCl-depleted *versus* normal diet

A NaCl-depleted diet was used in order to increase the number of renin-positive cells (Fig. 1). It is well known that NaCl restriction induces adaptive changes in the expression of ion channels and transporters (see, e.g. Masilamani *et al.* 2002). Therefore, side-by-side comparison of juxtaglomerular cells from rats with and without dietary NaCl restriction were made in single-channel experiments. No difference between the two preparations was found, demonstrating that the prominent appearance of Kir is not a consequence of the NaCl-restricted diet. Taking the evidence presented above together, we feel that the presence of Kir.2 on juxtaglomerular cells integrated in the rat afferent arteriole is established beyond reasonable doubt.

Isolated juxtaglomerular cells

At 2.8 mM K^{+} in the bath, the juxtaglomerular cells prepared from rat kidney have a resting membrane potential of −32 mV (Friis *et al.* 2003) and a similar value may be guessed for isolated mouse juxtaglomerular cells from published current–voltage relationship data (Friis *et al.* 1999, 2002). From these values it is obvious that there is no major contribution from a strongly inwardly rectifying K^{+} channel to the membrane potential, and one can only speculate why the channel is (essentially) inactive. It is possible that the procedure required for cell isolation might reduce the activity of the inwardly rectifying K^{+} channels. Alternatively, the integrity of the tissue, in particular coupling to neighbouring juxtaglomerular and smooth muscle cells via gap junctions to allow exchange of cellular metabolites, might be critical for the appearance of a prominent inwardly rectifying current. In addition, the channel, if it was active, may have been difficult to detect under the conditions used by Friis *et al.* (2003). According to the Goldman-Hodgkin-Katz current equation, inward potassium currents are rather small if physiological K^{+} concentrations (i.e. 2.8 mM) are used (Friis *et al.* 2003) rather than the high-K^{+} solution (142 mM) used here for the experiments in the voltage-clamp mode (Figs 2*B–D* and 3–6). The increase of the inwardly rectifying current with high K^{+} in the bath compared with standard PSS can be seen pretty well in Fig. 3.

Electrophysiological characterization

Inwardly rectifying K^{+} current. Voltage-dependent Ba^{2+} block. The IC_{50} value of ∼2 μM, determined for Ba^{2+} at a clamp potential of −100 mV, is in excellent agreement with results from native Kir2.x channels in rat cerebral arteries (Quayle *et al.* 1993), rat coronary arteries (Robertson *et al.* 1996), guinea-pig cardiomyocytes (Liu *et al.* 2001), parotid acinar cells (Hayashi *et al.* 2003) and trabecular meshwork cells (Llobet *et al.* 2001). As a voltage-independent value

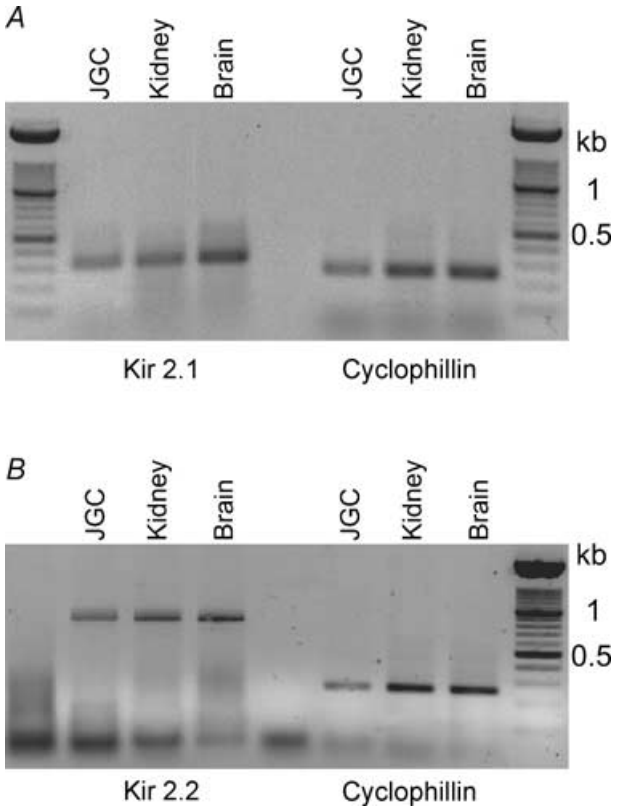

Figure 8. Detection of Kir2.x mRNA with RT-PCR
Presence of Kir2.1 (*A*) and Kir2.2 (*B*) mRNA in isolated juxtaglomerular cells (JGC), kidney and brain. Cyclophillin was used as house-keeping gene.

for sensitivity to Ba^{2+} block, the K_d value extrapolated to 0 mV, $K_d(0)$, is generally used. The value of 37 μM determined here is also in good agreement with values obtained in arterial smooth muscle cells (38.1 μM, Quayle *et al.* 1993; 21.1 μM, Robertson *et al.* 1996) and other tissues (Llobet *et al.* 2001; Hayashi *et al.* 2003). Finally, the value for the fraction of field sensed by Ba^{2+} at its binding site, $\delta = 0.39$, is in reasonable agreement with those determined in arterial smooth muscle cells (0.51 Robertson *et al.* 1996; 0.55 Quayle *et al.* 1993). Regarding the channel block by Ba^{2+}, this agreement shows that there is no difference between the inwardly rectifying K^+ channel in juxtaglomerular cells and arterial smooth muscle cells; in the latter cells, Kir2.1 is dominant (Bradley *et al.* 1999). Four Kir2 clones have been described (Kubo *et al.* 2002) and their Ba^{2+} sensitivity varies considerably (values at −100 mV: Kir2.1, 3.24 μM; Kir2.2, 0.51 μM; Kir2.3, 10.26 μM; Kir2.4, 235 μM; Liu *et al.* 2001). Although these values were determined at 60 mM K^+ in *Xenopus* oocytes and direct comparison with the results of this study must be made with care, it is conspicuous that the best agreement is found for Kir2.1.

Unitary conductance. In this study, a value of 31.5 pS was determined for the single-channel conductance of native channels in juxtaglomerular cells. Cloned Kir2 differ in their single-channel conductances, which are listed as 23, 34, 13 and 15 pS for Kir2.1, Kir2.2, Kir2.3 and Kir2.4, respectively (high symmetrical K^+, Kubo *et al.* 2002). The best agreement is found with Kir2.2 and the comparison seems to exclude Kir2.3 and Kir2.4 from being a major component of Kir2 in juxtaglomerular cells. However, reported values for Kir2.1 vary from 20 to 30 pS (Lopatin & Nichols, 2001), probably due to different expression systems and recording conditions. Furthermore, it was observed that the single-channel conductance values of Kir2.1 in the same preparation ranged from 2 to 33 pS, showing prominent scattering of the single-channel conductance for unknown reasons (Picones *et al.* 2001). With guinea pig Kir2.1 expressed in HEK293 cells, Liu *et al.* (2001) found a value of 30.6 ± 2.5 pS, which is very close to the value determined here and which was recorded under conditions similar to ours (mammalian cells, room temperature, cell-attached configuration, Hepes-buffered pipette solution with 140 mM K^+, 1 mM Ca^{2+} and 1 mM Mg^{2+}). Hence, the value determined here is well within the range reported for Kir2.1.

Other properties. Kir2.1 and 2.2 differ in their Cs^+ sensitivity and their inactivation properties. First, at −60 mV, Kir2.2 and 2.3 are almost completely blocked by 50 μM Cs^+ (Takahashi *et al.* 1994; Morishige *et al.* 1994) whereas inhibition is very small for Kir2.1 (Bradley *et al.* 1999 and references therein). Figure 3 shows no inhibition by Cs^+ (50 μM) at −60 mV. Second, Kir2.2 strongly inactivates at hyperpolarizing potentials whereas Kir2.1 does not (Takahashi *et al.* 1994). In Fig. 2*B*, there was a small inactivation of the current at the beginning of the experiment which was no longer seen at the end after washout of Ba^{2+}. Taken together, these points exclude a major contribution of Kir2.2 channels to the inwardly rectifying K^+ current in juxtaglomerular cells. Kir2.1 and 2.2 subunits can form heteromultimers (Kubo *et al.* 2002; Preisig-Müller *et al.* 2002); however, the weak inactivation and Cs^+ sensitivity of the current and the uniform single-channel conductance strongly suggest that Kir2.1 underlies the observed current in juxtaglomerular cells, although a (very) minor contribution of heteromultimers cannot be excluded.

Tedisamil and ciclazindol are K^+ channel blockers with limited specificity. Tedisamil is a bradycardic and anti-anginal agent possessing class III anti-arrhythmic activity and has been reported to block several potassium currents including the voltage activated current (I_{Kv}), the calcium-activated potassium current ($I_{K,Ca}$), as well as the ATP-sensitive current $I_{K,ATP}$ at concentations < 10 μM (Barrett *et al.* 2001 and references therein). Ciclazindol is an inhibitor of $I_{K,ATP}$ at concentrations < 10 μM and of I_{Kv} at concentrations up to 100 μM (Green *et al.* 1996). We found here that at 100 μM, these drugs inhibited the inwardly rectifying K^+ current (Kir2.1) by 30 and 50%, adding to the low selectivity profile of these compounds.

Depolarization-activated channel. In cell-attached patches a big (∼180 pS) channel was often observed at potentials positive to +40 mV (K^+-rich buffer in the bath) or +80 mV (Na^+-rich buffer in the bath). Although this channel was not characterized in detail, the high conductance in a solution where K^+ and Cl^- are the dominating small ions on both sides of the membrane, together with the reversal potential, which agreed with that of the Kir2 channel, point to a potassium channel. Moreover, the high conductance and the fact that the depolarization threshold required for channel activation was reduced when cells were bathed in the high-K^+, Ca^{2+}-containing solution point to the calcium-sensitive voltage-gated K^+ channel of large conductance BK_{Ca} ($K_{Ca}1.1$). The presence of a cAMP-sensitive splice variant of this channel in isolated juxtaglomerular cells has recently been shown by Friis *et al.* (2003). In our preparation, this channel does not contribute to membrane potential at rest since no activity was detected in cell-attached patches at negative membrane potentials.

Immunocytochemistry and PCR

Collectively, the electrophysiological results showed a dominating role of Kir2.1 in the inwardly rectifying current in juxtaglomerular cells. This conclusion is supported by

the detection of Kir2.1 but not Kir2.2 in the distal part of the afferent arteriole using specific antibodies (Fig. 7); controls in brain showed that the Kir2.2 antibody was functional. On the other hand, in isolated juxtaglomerular cells, there were signals for Kir2.1 and Kir2.2 mRNA in the PCR analyses (Fig. 8) pointing at a discrepancy between mRNA and protein levels. However, PCR analysis was not quantitative and the amount of Kir2.2 protein may have been below the detection level of the antibody.

Physiological importance of the inward current for juxtaglomerular cells

Following on from the work of Kurtz & Penner (1989), we have characterized here an inwardly rectifying K^+ conductance in rat juxtaglomerular cells. Electrophysiological, immunocytochemical and PCR experiments show that, as in vascular smooth muscle, Kir2.1 is the dominating or even exclusive channel subtype underlying this conductance. Block of this channel by Ba^{2+} (this study) or angiotensin II (Kurtz & Penner, 1989) strongly depolarizes the cell, showing that this conductance is a determinant of the resting membrane potential of juxtaglomerular cells. In the rat at least, juxtaglomerular cells are endowed with L-type voltage-dependent Ca^{2+} channels (Friis *et al.* 2003) and the cytoplasmic Ca^{2+} concentration is a major (negative) regulator of renin secretion (reviews in Kurtz, 1989; Skøtt *et al.* 1991; Osswald & Quast, 1995; Persson, 2003). Hence, the inwardly rectifying conductance in juxtaglomerular cells is directly involved in the control of renin secretion and thereby in homeostasis of salt and water and the control of blood pressure.

References

Albinus M, Finkbeiner E, Sosath B & Osswald H (1998). Isolated superfused juxtaglomerular cells from rat kidney: a model for study of renin secretion. *Am J Physiol (Renal Physiol)* **275**, F991–F997.

Barrett TD, Hennan JK, Fischbach PS, O'Neill BP, Driscoll EM Jr & Lucchesi BR (2001). Tedisamil and dofetilide-induced torsades de pointes, rate and potassium dependence. *Br J Pharmacol* **132**, 1493–1500.

Bradley KK, Jaggar JH, Bonev AD, Heppner TJ, Flynn ERM, Nelson MT & Horowitz B (1999). $K_{ir}2.1$ encodes the inward rectifier potassium channel in rat arterial smooth muscle cells. *J Physiol* **515**, 639–651.

Bührle CP, Nobiling R, Mannek E, Schneider D, Hackenthal E & Taugner R (1984). The afferent glomerular arteriole: immunocytochemical and electrophysiological investigations. *J Cardiovasc Pharmacol* **6**, S383–S393.

Bührle CP, Nobiling R & Taugner R (1985). Intracellular recordings from renin-positive cells of the afferent glomerular arteriole. *Am J Physiol (Renal Physiol)* **249**, F272–F281.

Cantin M, Araujo-Nascimento M-F, Benchimol S & Desormeaux Y (1977). Metaplasia of smooth muscle cells into juxtaglomerular cells in the juxtaglomerular apparatus, arteries, and arterioles of the ischemic (endocrine) kidney. An ultrastructural-cytochemical and autoradiographic study. *Am J Pathol* **87**, 581–602.

Fishman MC (1976). Membrane potential of juxtaglomerular cells. *Nature* **260**, 542–544.

Friis UG, Jensen BL, Aas JK & Skøtt O (1999). Direct demonstration of exocytosis and endocytosis in single mouse juxtaglomerular cells. *Circ Res* **84**, 929–936.

Friis UG, Jensen BL, Sethi S, Andreasen D, Hansen PB & Skøtt O (2002). Control of renin secretion from rat juxtaglomerular cells by cAMP-specific phosphodiesterases. *Circ Res* **90**, 996–1003.

Friis UG, Jørgensen F, Andreasen D, Jensen BL & Skøtt O (2003). Molecular and functional identification of cyclic AMP-sensitive BK_{Ca} potassium channels (ZERO variant) and L-type voltage-dependent calcium channels in single rat juxtaglomerular cells. *Circ Res* **93**, 213–220.

Green M, Edwards G, Kirkup AJ, Miller M & Weston A (1996). Pharmacological charakterization of the inwardly-rectifying current in the smooth muscle cells of the rat bladder. *Br J Pharmacol* **119**, 1509–1518.

Hackenthal E, Paul M, Ganten D & Taugner R (1990). Morphology, physiology, and molecular biology of renin secretion. *Physiol Rev* **70**, 1067–1116.

Hamill OP, Marty A, Neher E, Sakmann B & Sigworth FJ (1981). Improved patch-clamp techniques for high-resolution current recording from cells and cell-free membrane patches. *Pflugers Arch* **391**, 85–100.

Hayashi M, Komazaki S & Ishikawa T (2003). An inwardly rectifying K^+ channel in bovine parotid acinar cells: possible involvement of Kir2.1. *J Physiol (Lond)* **547**, 255–269.

Kubo Y, Adelman JP, Clapham DE, Jan LY, Karschin A, Kurachi Y, Lazdunski M, Lester HA, Nichols CG, Seino S & Vandenberg CA (2002). Potassium channels K_{ir}. In *The IUPHAR Compendium of Voltage-Gated Ion Channels*, ed. Catterall WA, Chandy KG & Gutman GA, pp. 154–171. IUPHAR Media, Leeds, UK.

Kurtz A (1989). Cellular control of renin secretion. *Rev Physiol Biochem Pharmacol* **113**, 1–40.

Kurtz A & Penner R (1989). Angiotensin II induces oscillations of intracellular calcium and blocks anomalous inward rectifying potassium current in mouse renal juxtaglomerular cells. *Proc Natl Acad Sci U S A* **86**, 3423–3427.

Kurtz A, Skøtt O, Chegini S & Penner R (1990). Lack of direkt evidence for a functional role of voltage-operated calcium channels in juxtaglomerular cells. *Pflugers Arch* **416**, 281–287.

Liu GX, Derst C, Schlichthörl G, Heinen S, Seebohm G, Bruggemann A, Kummer W, Veh RW, Daut J & Preisig-Müller R (2001). Comparison of cloned Kir2 channels with native inward rectifier K^+ channels from guinea-pig cardiomyocytes. *J Physiol* **532**, 115–126.

Llobet A, Gasull X, Palés J, Martí E & Gual A (2001). Identification of Kir2.1 channel activity in cultured trabecular meshwork cells. *Invest Ophthalmol Vis Sci* **42**, 2371–2379.

Lopatin AN & Nichols CG (2001). Inward rectifiers in the heart: an update on I_{K1}. *J Mol Cell Cardiol* **33**, 625–638.

Masilamani S, Wang X, Kim G-H, Brooks H, Nielsen J, Nielsen S, Nakamura K, Stokes JB & Knepper MA (2002). Time course of renal Na-K-ATPase, NHE3, NKCC2, NCC, and ENaC abundance changes with dietary NaCl restriction. *Am J Physiol (Renal Physiol)* **283**, F648–F657.

Metzger F & Quast U (1996). Binding of [^{3}H]-P1075, an opener of ATP-sensitive K^+ channels, to rat glomerular preparations. *Naunyn-Schmiedeberg's Arch Pharmacol* **354**, 452–459.

Morishige KI, Takahashi N, Jahangir A, Yamada M, Koyama H, Zanelli JS & Kurachi Y (1994). Molecular cloning and functional expression of a novel brain specific inward rectifier potassium channel. *FEBS Lett* **346**, 251–256.

Neher E (1992). Correction for liquid junction potentials in patch clamp experiments. *Meth Enzymol – Ion Channels* **207**, 123–131.

Osswald H & Quast U (1995). Ion channels and renin secretion from juxtaglomerular cells. In *The Electrophysiology of Neuroendocrine Cells*, ed. Scherübl H & Hescheler J, pp. 301–314. CRC Press, Boca Raton, FL, USA.

Persson PB (2003). Renin: origin, secretion and synthesis. *J Physiol* **552**, 667–671.

Pfaff IL, Wagner H-J & Vallon V (1999). Immunolocalization of protein kinase C isoenzymes α, βI and βII in rat kidney. *J Am Soc Nephrol* **10**, 1861–1873.

Picones A, Keung E & Timpe LC (2001). Unitary conductance variation in Kir2.1 and in cardiac inward rectifier potassium channels. *Biophys J* **81**, 2035–2049.

Preisig-Müller R, Schlichthörl G, Goerge T, Heinen S, Brüggemann A, Rajan S, Derst C, Veh RW & Daut J (2002). Heteromerization of Kir2.x potassium channels contributes to the phenotype of Andersen's syndrome. *Proc Natl Acad Sci U S A* **99**, 7774–7779.

Prüss H, Wenzel M, Eulitz D, Thomzig A, Karschin A & Veh RW (2003). Kir2 potassium channels in rat striatum are strategically localized to control basal ganglia function. *Mol Brain Res* **110**, 203–219.

Quayle JM, McCarron JG, Brayden JE & Nelson MT (1993). Inward rectifier K^+ currents in smooth muscle cells from rat resistance-sized cerebral arteries. *Am J Physiol (Cell Physiol)* **265**, C1363–C1370.

Robertson BE, Bonev AD & Nelson MT (1996). Inward rectifier K^+ currents in smooth muscle cells from rat coronary arteries: block by Mg^{2+}, Ca^{2+}, and Ba^{2+}. *Am J Physiol (Heart Circ Physiol)* **271**, H696–H705.

Russ U, Rauch U & Quast U (1999). Pharmacological evidence for a K_{ATP} channel in renin-secreting cells from rat kidney. *J Physiol (Lond)* **517**, 781–790.

Scholz H & Kurtz A (1995). Differential regulation of cytosolic calcium between afferent arteriolar smooth muscle cells from mouse kidney. *Pflugers Arch* **431**, 46–51.

Sequeira Lopez ML, Pentz ES, Robert B, Abrahamson DR & Gomez RA (2001). Embryonic origin and lineage of juxtaglomerular cells. *Am J Physiol (Renal Physiol)* **281**, F345–F356.

Skøtt O, Salomonsson M, Persson AEG & Jensen BL (1991). Mechanisms of renin release from juxtaglomerular cells. *Kidney Intsupplement* **32**, S16–S19.

Takahashi N, Morishige KI, Jahangir A, Yamada M, Koyama H & Kurachi Y (1994). Molecular cloing and functional expression of cDNA encoding a second class of inward rectifier potassium channels in the mouse brain. *J Biol Chem* **269**, 23274–23279.

Taugner R & Hackenthal E (1989). *The Juxtaglomerular Apparatus*. Springer-Verlag, Berlin Heidelberg New York.

Thomzig A, Prüss H & Veh RW (2003). The Kir6.1-protein, a pore-forming channels, is prominently expressed subunit of ATP-sensitive potassium by giant cholinergic interneurons in the striatum of the rat brain. *Brain Res* **986**, 132–138.

Thomzig A, Wenzel M, Karschin C, Eaton MJ, Skatchkov SN, Karschin A & Veh RW (2001). Kir6.1 is the principal pore-forming subunit of astrocyte but not neuronal plasma membrane K-ATP channels. *Mol Cellular Neuroscience* **18**, 671–690.

Woodhull AM (1973). Ionic blockage of sodium channels in nerve. *J Ge Physiol* **61**, 687–708.

Acknowledgements

This study was supported by the Interdisciplinary Centre for Clinical Research (IZKF) Tübingen (Fö 01KS 9602) and by a grant from the Deutsche Forschungsgemeinschaft (Ve 187/1–3) to R.W.V.

Supplementary material

The online version of this paper can be accessed online at:
DOI: 10.1113/jphysiol.2004.070359
http://jp.physoc.org/cgi/content/full/jphysiol.2004.070359DC1
and contains two supplementary figures.
This material can also be found at:
http://www.blackwellpublishing.com/products/journals/suppmat/tjp/tjp478/tjp478sm.htm